Modern Physics Letters B
Vol. 35, No. 26 (2021) 2150449 (9 pages)

DOI: 10.1142/S0217984921504492

Lump and rational solutions for weakly coupled generalized Kadomtsev–Petviashvili equation

Hongyu Wu* and Jinxi Fei

Department of Photoelectric Engineering, Lishui University,
Lishui 323000, China
**hongyuwulsu@163.com*

Wenxiu Ma

Department of Mathematics and Statistics,
University of South Florida, Tampa, FL 33620-5700, USA
Department of Mathematics, Zhejiang Sci-Tech University, Hangzhou 310018, China
Department of Mathematics, Zhejiang Normal University, Jinhua 321004, China
Department of Mathematics, King Abdulaziz University, Jeddah, Saudi Arabia
School of Mathematics, South China University of Technology,
Guangzhou 510640, China
College of Mathematics and Systems Science,
Shandong University of Science and Technology,
Qingdao 266590, Shandong, China
Department of Mathematical Sciences, North-West University,
Mafikeng Campus, Private Bag X2046, Mmabatho 2735, South Africa
mawx@cas.usf.edu

Received 11 May 2021
Revised 6 July 2021
Accepted 12 July 2021
Published 16 August 2021

Through the Z_m-KP hierarchy, we present a new $(3+1)$-dimensional equation called weakly coupled generalized Kadomtsev–Petviashvili (wc-gKP) equation. Based on Hirota bilinear differential equations, we get rational solutions to wc-gKP equation, and further we obtain lump solutions by searching for a symmetric positive semi-definite matrix. We do some numerical analysis on the trajectory of rational solutions and fit the trajectory equation of wave crest. Some graphics are illustrated to describe the properties of rational solutions and lump solutions. The method used in this paper to get lump solutions by constructing a symmetric positive semi-definite matrix can be applied to other integrable equations as well. The results expand the understanding of lump and rational solutions in soliton theory.

Keywords: Wc-gKP equation; symmetric positive semi-definite matrix; lump solutions; rational solutions.

*Corresponding author.

1. Introduction

Nonlinear science plays an important role in fluid mechanics, plasma physics and other fields.[1–4] The nonlinear evolution equation can explain the movement of fluid in shallow water waves well.[3–10] Therefore, finding the exact solution of these integrable systems is a very significant work. In recent years, experts in physics and fluid mechanics have, for wave propagation in integrable systems, extended the generation mechanism and dynamic properties of rogue waves and lump waves.[1–10]

In this paper, we consider the (3+1)-dimensional generalized Kadomtsev–Petviashvili (KP) equation[11] as follows:

$$u_{xt} - u_{xxxy} - 3(u_x u_y)_x - 2u_{xx} + u_{yy} + u_{zz} = 0, \tag{1}$$

which is derived from the generalized bilinear equation. Here, $u = u(x, y, z, t)$ denotes a scalar function of the space variables x, y, z, and time variable t.

Under the variable transformation, we have

$$u(x, y, z, t) = 2(\ln f)_x, \tag{2}$$

where $f(x, y, z, t)$ is a real function. Inserting Eq. (2) into Eq. (1) yields

$$(D_x D_t - D_x^3 D_y - 2D_x^2 + D_y^2 + D_z^2) f \cdot f = 0. \tag{3}$$

The operator D is Hirota's bilinear differential operator defined by

$$D_x^m D_t^n f \cdot g = \left(\frac{\partial}{\partial x} - \frac{\partial}{\partial x'}\right)^m \left(\frac{\partial}{\partial t} - \frac{\partial}{\partial t'}\right)^n f(x, y, z, t) \cdot g(x, y, z, t)|_{x'=x, t'=t}. \tag{4}$$

Through the Z_m-KP hierarchy which takes values in a maximal commutative subalgebra,[12,13] a new $(3+1)$-dimensional equation called weakly coupled generalized Kadomtsev–Petviashvili (wc-gKP) is presented:

$$\begin{cases} u_{xt} - u_{xxxy} - 3(u_x u_y)_x - 2u_{xx} + u_{yy} + u_{zz} = 0 \\ v_{tx} - v_{xxxy} - 3(v_x u_y)_x - 3(u_x v_y)_x - 2v_{xx} + v_{yy} + v_{zz} = 0. \end{cases} \tag{5}$$

In addition, the consistent Riccati expansion method, generalized bilinear method and other ways can also be used to construct the new nonlinear systems which possess the rational and lump solutions.[14–18]

The $(3+1)$-dimensional equation (5) reduces to the following equation in $(2+1)$ dimensions under $z = x$:

$$\begin{cases} u_{xt} - u_{xxxy} - 3(u_x u_y)_x - u_{xx} + u_{yy} = 0, \\ v_{tx} - v_{xxxy} - 3(v_x u_y)_x - 3(u_x v_y)_x - v_{xx} + v_{yy} = 0. \end{cases} \tag{6}$$

In most studies on the lump solutions, the bulk of Refs. 19–25 get lump solutions to a single equation by searching for positive quadratic functions.[1–10] Lump and rational solutions also can be generated from soliton solutions by taking a long wave limit.[29,30] In particular, Tian *et al.* use these two methods to investigate the breather wave and the lump wave of the KP equation.[26–28] In this paper, we try to find lump and rational solutions of Eq. (6) by searching for the symmetric positive semi-definite matrix. Furthermore, we discuss the trajectory of lump and rational solutions, and do some numerical analysis on rational solutions to Eq. (6).

The arrangement of this paper is organized as follows. In Sec. 2, we construct the bilinear equation to Eq. (6). In Sec. 3, based on the bilinear formalism to Eq. (6), we get rational solutions to Eq. (6), and further we obtain lump solutions by searching for a symmetric positive semi-definite matrix. We also do some numerical analysis on the trajectory of rational solutions and fit the trajectory equation of the wave crest. Finally, some conclusions are given in Sec. 4.

2. Bilinear Formalism

Using the variable transformation, we have

$$\begin{cases} u = 2(\ln f)_x, \\ v = 2\left(\dfrac{g}{f}\right)_x, \end{cases} \tag{7}$$

the bilinear form of Eq. (6) is generated as

$$\begin{cases} (D_x D_t - D_x^3 D_y - D_x^2 + D_y^2) f \cdot f = 0, \\ (D_x D_t - D_x^3 D_y - D_x^2 + D_y^2) f \cdot g = 0. \end{cases} \tag{8}$$

That is,

$$\begin{cases} 2f_{tx} f - 2f_{xx} f - 2f_{xxxy} f + 2f_{yy} f - 2f_x f_t + 2{f_x}^2 + 6f_{xxy} f_x - 6f_{xx} f_{xy} \\ \quad + 2f_{xxx} f_y - 2{f_y}^2 = 0, \\ f g_{tx} - f g_{xx} - f g_{xxxy} + f g_{yy} + f_{tx} g - f_{xx} g - f_{xxxy} g + f_{yy} g - f_t g_x \\ \quad - f_x g_t + 2 f_x g_x + 3 f_x g_{xxy} - 3 f_{xx} g_{xy} + f_{xxx} g_y \\ \quad + 3 f_{xxy} g_x - 3 f_{xy} g_{xx} + f_y g_{xxx} - 2 f_y g_y = 0. \end{cases} \tag{9}$$

Here, $f = f(x,y,t)$, $g = g(x,y,t)$ are real functions, and the operator D is Hirota's bilinear differential operator defined by Eq. (4).

It is clear that if f, g solve Eq. (9), then $u(x,y,t)$, $v(x,y,t)$ are solutions to Eq. (6) through dependent variable transformation equations (7).

3. Rational Solutions and Lump Solutions

In order to find the rational solutions to Eq. (6), we make the following assumption:

$$\begin{cases} f = X^T A X + c_1, \\ g = X^T B X + c_2, \end{cases} \tag{10}$$

and

$$A = \begin{bmatrix} a_{11} & a_{12} & a_{13} \\ a_{12} & a_{22} & a_{23} \\ a_{13} & a_{23} & a_{33} \end{bmatrix}, \quad B = \begin{bmatrix} b_{11} & b_{12} & b_{13} \\ b_{12} & b_{22} & b_{23} \\ b_{13} & b_{23} & b_{33} \end{bmatrix}, \quad X = \begin{bmatrix} x \\ y \\ t \end{bmatrix}. \tag{11}$$

Here, both A and B are symmetric matrices with real entries. c_1, c_2 are also real parameters to be determined.

Substituting Eq. (10) into Eqs. (9) and (12) can be derived by comparing the coefficients of the same power terms of x, y, and t. The following set of constraining equations for the parameters had been generated by performing a direct Maple symbolic computation with f:

$$\begin{aligned}
&c_1 = c_1, \quad a_{11} = a_{11}, \quad a_{12} = a_{12},\\
&a_{13} = \frac{3{a_{11}}^2 a_{12} + {a_{11}}^2 c_1 - {a_{12}}^2 c_1}{a_{11} c_1},\\
&a_{22} = \frac{a_{12}(3{a_{11}}^2 + a_{12} c_1)}{a_{11} c_1},\\
&a_{23} = -\frac{a_{12}(3{a_{11}}^2 a_{12} - {a_{11}}^2 c_1 + {a_{12}}^2 c_1)}{{a_{11}}^2 c_1},\\
&a_{33} = \frac{9{a_{11}}^4 {a_{12}}^2 + 6{a_{11}}^4 a_{12} c_1 + {a_{11}}^4 {c_1}^2 + 6{a_{11}}^2 {a_{12}}^3 c_1 - 2{a_{11}}^2 {a_{12}}^2 {c_1}^2 + {a_{12}}^4 {c_1}^2}{{a_{11}}^3 {c_1}^2}.
\end{aligned} \tag{12}$$

Combining Eqs. (7), (10) and (12), we can get the f

$$\begin{aligned}
f = {} & a_{11} x^2 + 2a_{12} xy + \frac{(6{a_{11}}^2 a_{12} + 2{a_{11}}^2 c_1 - 2{a_{12}}^2 c_1) xt}{a_{11} c_1}\\
& + \frac{a_{12}(3{a_{11}}^2 + a_{12} c_1) y^2}{a_{11} c_1} - 2\frac{a_{12}(3{a_{11}}^2 a_{12} - {a_{11}}^2 c_1 + {a_{12}}^2 c_1) yt}{{a_{11}}^2 c_1}\\
& + \frac{\begin{gathered}(9{a_{11}}^4 {a_{12}}^2 + 6{a_{11}}^4 a_{12} c_1 + {a_{11}}^4 {c_1}^2 + 6{a_{11}}^2 {a_{12}}^3 c_1\\ - 2{a_{11}}^2 {a_{12}}^2 {c_1}^2 + {a_{12}}^4 {c_1}^2) t^2\end{gathered}}{{a_{11}}^3 {c_1}^2} + c_1,
\end{aligned} \tag{13}$$

that corresponds to the rational solutions u to Eq. (6). To get lump solutions u to Eq. (6), the matrix A and parameter c_1 should satisfy the following constraints: (1) Matrix A is a positive semi-definite matrix, in other words, the eigenvalues of matrix A are all non-negative. (2) $c_1 > 0$. (3) The elements in matrix A must also satisfy the constraints $a_{11} > 0$ and $a_{11} a_{22} - a_{12}^2 > 0$. Conditions (1) and (2) guarantee that f is always greater than 0. Condition (3) guarantees that f has only one minimum value for any time t.

It is found that there are three arbitrary parameters a_{11}, a_{12}, c_1 in Eq. (13). Under the constraints of the above three conditions, we may assign the values of the three free variables as follows:

$$a_{11} = 1, \quad a_{12} = 1, \quad c_1 = 1, \tag{14}$$

which implies that

$$f = 21t^2 + 6xt - 6yt + x^2 + 2xy + 4y^2 + 1, \tag{15}$$

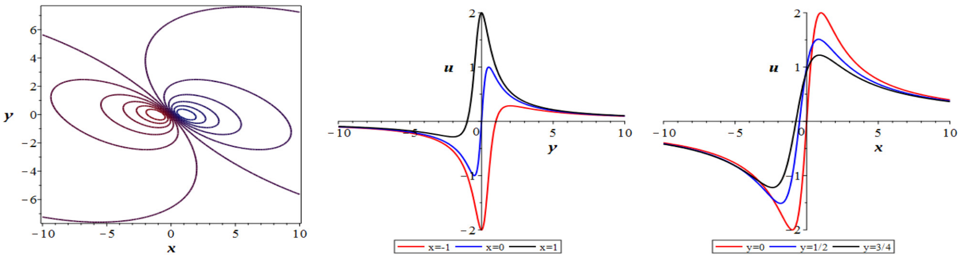

(a) (b) (c)

Fig. 1. (Color online) The lump solution u (Eq. (16) to Eq. (6)) at $t = 0$. (a) Contour plot; (b) x-curve; (c) y-curve.

and

$$u = \frac{12t + 4x + 4y}{21t^2 + 6xt - 6yt + x^2 + 2xy + 4y^2 + 1}. \tag{16}$$

The contour plot, x-curve, and y-curve of the lump solution u are depicted in Fig. 1 when $t = 0$. Lump solution u has a maximum point $(-5t + 1, 2t)$ and a minimum point $(-5t - 1, 2t)$, and the corresponding maxima and minima are 2 and -2, respectively. The moving velocity of both extremum points with time is $\sqrt{29}$.

Although the constraints between parameters $\{a_{ij}, b_{ij}, c_1, c_2, i, j = 1, 2, 3\}$ can be obtained by substituting Eq. (13) and $g = X^T BX + c_2$ into Eq. (9), the constraint equations are too complex to further analyze the properties of the rational solutions v. To remedy this, we substitute Eq. (15) into Eq. (9) and get the following constraint equations:

$$\begin{aligned}
&b_{11} = b_{11}, \quad b_{12} = b_{12}, \quad b_{13} = -3c_2 + b_{12} + 5b_{11},\\
&b_{22} = -3c_2 + 5b_{12} + 2b_{11}, \quad b_{23} = 3c_2 - 8b_{12} + 2b_{11},\\
&b_{33} = -30c_2 + 42b_{12} + 9b_{11}, \quad c_2 = c_2.
\end{aligned} \tag{17}$$

Equation (17) contains three arbitrary parameters b_{11}, b_{12}, c_2, which are given as follows:

$$b_{11} = 1, \quad b_{12} = 2, \quad c_2 = 1, \tag{18}$$

which implies that

$$g = 63t^2 + 8tx - 22ty + x^2 + 4xy + 9y^2 + 1, \tag{19}$$

and

$$v_r = \frac{\begin{aligned}&-2x^2y - 2x^2t - 10xy^2 + 32xyt - 84xt^2 - 2y^3 - 2y^2t\\ &+ 42yt^2 - 210t^3 + 2y + 2t\end{aligned}}{(21t^2 + 6tx - 6ty + x^2 + 2xy + 4y^2 + 1)^2}. \tag{20}$$

Here, v_r is the rational solution to Eq. (6). Equations (16) and (20) are a set of rational solutions to Eq. (6).

Table 1. The position of the crest of rational solution v_r.

t	x	y	h	$v_{r,x}$	$v_{r,y}$
10	−50.00333918	20.01010358	60.00991274	−0.012038487	−0.028698477
20	−100.0016729	40.00509711	120.0020929	−0.019203938	−0.046050917
30	−150.0011160	60.00340827	179.9966164	−0.021803249	−0.052418889
40	−200.0008373	80.00256004	239.9965202	−0.023218168	−0.055863414
50	−250.0006700	100.0020499	299.9961000	−0.023990630	−0.057860924
60	−300.0005584	120.0017093	359.9974186	−0.024484116	−0.059487168
70	−350.0004786	140.0014657	419.9449314	−0.025010567	−0.059773932
80	−400.0004188	160.0012829	479.9265658	−0.025218182	−0.058815766
90	−450.0003723	180.0011407	540.0522814	−0.025904692	−0.061256340
100	−500.0003351	200.0010268	600.0720536	−0.026319387	−0.063187144

We find that rational solution v_r has some interesting properties. First of all, v_r is an odd function, which means that $v(x, y, t) + v(-x, -y, -t) = 0$. So, if we can figure out the trajectory of the crest when $t > 0$, we can figure out where the crest is at any given moment. Second, the solutions obtained from equations $v_{r,x} = 0$ and $v_{r,y} = 0$ are unwieldy algebraic structures. From that we can be sure that the crest is not moving uniformly in a straight line with time. Therefore, in order to study the motion path of the crest clearly, some numerical analysis on rational solutions is appropriate.

Table 1 describes the position of the crest at different moments. Here, h is the height of the crest, and $v_{r,x}, v_{r,y}$ are used to measure the error of the numerical calculation. The closer $v_{r,x}$ and $v_{r,y}$ are to 0, the more accurate the position of the calculated crest is.

According to the description in the previous paragraph, we conduct nonlinear fitting for the data in Table 1. In some time range of $t > 0$, the movement trajectory of the wave crest roughly conforms to the following equation:

$$\begin{cases} x = \dfrac{-0.0335241199228886}{t + 0.0396119992712996} - 5t, \\ y = \dfrac{0.102865205001053}{t + 0.181067231314590} + 2t, \end{cases} \tag{21}$$

and, the height of wave crest h satisfies the following equation:

$$h = -0.0141135773333083 + 6.00024659784242t. \tag{22}$$

It can be known from Eq. (21) that with the increase of time, the motion rule of wave crest is approximately uniform linear motion. In addition, every other unit of time, at the height of the crest, increases by about six. It is worth mentioning that although the height of the crest changes over time, the lump wave is always local in the $x - o - y$ plane. Figure 2 shows this feature intuitively and clearly. From Fig. 2, we can intuitively observe that v_r is an odd function, which has been discussed previously. Combined with Eq. (21), we can get the trajectory of the minimum

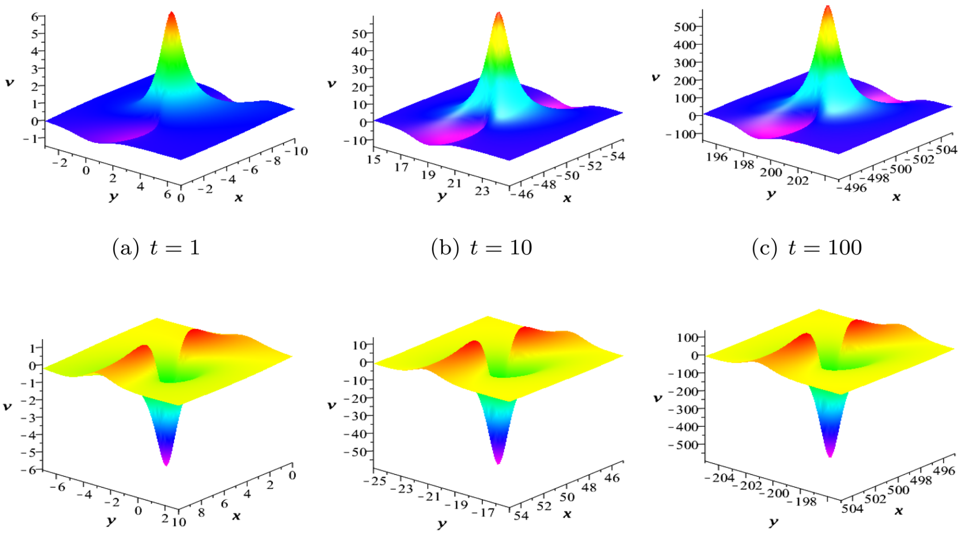

(a) $t = 1$ (b) $t = 10$ (c) $t = 100$

(d) $t = -1$ (e) $t = -10$ (f) $t = -100$

Fig. 2. (Color online) The rational solution v_r (Eq. (20) to Eq. (6)).

point when $t < 0$

$$\begin{cases} x = \dfrac{-0.0335241199228886}{t - 0.0396119992712996} - 5t, \\[2ex] y = \dfrac{0.102865205001053}{t - 0.181067231314590} + 2t. \end{cases} \tag{23}$$

When $t > 0$, the height of the wave peak increases with the increase of time, this qualitative conclusion conforms to Eq. (22). In addition, it can be clearly seen from Fig. 2 that rational solution v_r does not change its shape significantly with time t. Rational solution v_r looks particularly similar to the spatial structures of lump solutions.

Whether Eqs. (21) and (23) can accurately express the position of the wave peak at other moments, we have made the following test on Eqs. (21) and (23), and the results are shown in Table 2.

Table 2. Test of fitting equations.

t	x	y	h	$v_{r,x}$	$v_{r,y}$
700	−3500.000048	1400.000147	4172.000294	−0.022112116	0.008479364
800	−4000.000042	1600.000129	4798.000258	−0.029704090	0.003799510
900	−4500.000037	1800.000114	5380.000228	−0.017040070	−0.098400384
−700	3500.000048	−1400.000147	−4172.000294	−0.022112116	0.008479364
−800	4000.000042	−1600.000129	−4798.000258	−0.029704090	0.003799510
−900	4500.000037	−1800.000114	−5380.000228	−0.017040070	−0.098400384

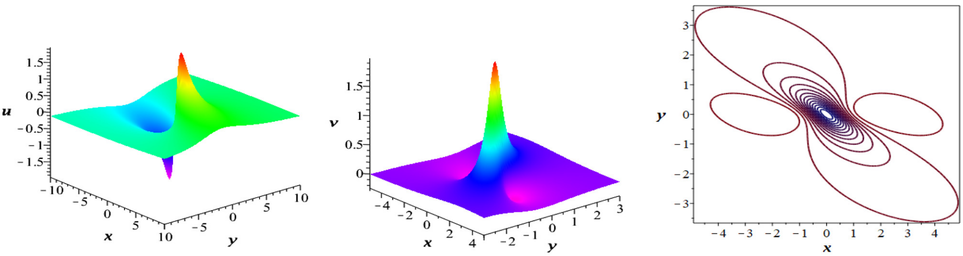

(a) (b) (c)

Fig. 3. (Color online) Lump solutions u and v (Eq. (24) to Eq. (6)) at $t = 0$. (a) Lump solution u. (b) Lump solutions v. (c) Contour plot of lump solution v.

In Table 2, both $v_{r,x}$ and $v_{r,y}$ are very close to 0, so Eqs. (21) and (23) can accurately represent the position of wave peaks when $t \in [-900, 900]$. From Table 2, we can also find that Eq. (22) is no longer able to accurately express the height of the wave peak, but we can still calculate the height of the wave peak through Eqs. (20), (21) and (23).

Finally, we give a class of lump solutions to Eq. (6). If $u = 2(\ln f)_x$ is a lump solution to Eq. (6) and $g = f_x$, then $v = 2(\frac{g}{f})_x$ is also a lump solution to Eq. (6). In combination with Eqs. (13) and (14), we give a specific set of solutions to Eq. (6):

$$\begin{cases} u = \dfrac{12t + 4x + 4y}{21t^2 + 6xt - 6yt + x^2 + 2xy + 4y^2 + 1}, \\ v = \dfrac{6t^2 - 12tx - 36ty - 2x^2 - 4xy + 4y^2 + 2}{(21t^2 + 6tx - 6ty + x^2 + 2xy + 4y^2 + 1)^2}. \end{cases} \tag{24}$$

Lump solution u has a maximum point $(-5t + 1, 2t)$ and a minimum point $(-5t - 1, 2t)$, and the corresponding maxima and minima are 2 and -2, respectively. At any given moment, the peak of lump solution v is in position $(-5t, 2t)$. Lump wave u and lump wave v move at the same speed with time, both of which are $\sqrt{29}$. This type of lump wave is illustrated in Fig. 3.

4. Conclusion

In this work, we obtain rational solutions and lump solutions to wc-gKP equations by using bilinear formalism and constructing symmetric positive semi-definite matrices. We also find an interesting set of rational solutions u, v_r to Eq. (6), as shown in Eqs. (15) and (20). Figure 2 shows that the rational solution v_r is an odd function, and the spatial structure of v_r is very similar to that of general lump solutions. With the increase of time, the motion trajectory equations (21) and (24) of v_r are approximately uniform linear motion, and the height equation (22) of the crest increases linearly. In the same way, we can get rational and lump solutions to Eq. (5). The method used in this paper to get lump solutions by constructing a symmetric positive semi-definite matrix can be applied to other integrable equations as well. Whether general higher-order lump solutions can be obtained by constructing symmetric positive semi-definite matrices is an important direction of our future research. Meanwhile, we also hope that our results will provide some valuable information in the field of nonlinear science.

Acknowledgment

This work is supported by the National Natural Science Foundation of China under Grant No. 11775104.

References

1. W. X. Ma and L. Q. Zhang, *Pramana-J. Phys.* **94** (2020) 43.
2. X. L. Yong, W. X. Ma, Y. H. Wang and Y. Liu, *Comput. Math. Appl.* **75** (2018) 3414.
3. F. D. Wang and W. X. Ma, *Mod. Phys. Lett. B* **34** (2020) 2050197.
4. S. Batwa and W. X. Ma, *Front. Math. China* **15** (2020) 435.
5. S. T. Chen and W. X. Ma, *Front. Math. China* **13** (2018) 525.
6. S. Batwa and W. X. Ma, *Adv. Math. Phys.* **2018** (2018) 2062398.
7. Y. L. Sun, W. X. Ma and J. P. Yu, *Math. Method. Appl. Sci.* **43** (2020) 6276.
8. L. Y. Ding, W. X. Ma and Q. X. Chen, *Appl. Math. Lett.* **112** (2021) 106809.
9. L. Q. Zhang, W. X. Ma and Y. H. Huang, *Adv. Math. Phys.* **2020** (2020) 3542320.
10. S. Manukure, Y. Zhou and W. X. Ma, *Comput. Math. Appl.* **75** (2018) 2414.
11. J. P. Yu and Y. L. Sun, *Nonlinear Dyn.* **87** (2015) 2755.
12. I. A. B. Strachan and D. Zuo, *J. Math. Phys.* **56** (2015) 219.
13. C. Li, *J. Phys. A-Math. Gen.* **49** (2016) 015203.
14. B. Ren, J. Lin and Z. M. Lou, *Appl. Math. Lett.* **105** (2020) 106326.
15. B. Ren, J. Lin and J. Yu, *Mod. Phys. Lett. B* **34** (2020) 2050215.
16. B. Ren, W. X. Ma and J. Yu, *Nonlinear Dyn.* **96** (2019) 717.
17. J. P. Yu and Y. L. Sun, *Nonlinear Dyn.* **87** (2017) 1405.
18. J. P. Yu and Y. L. Sun, *Nonlinear Dyn.* **90** (2017) 2263.
19. W. X. Ma, *Phys. Lett. A.* **379** (2015) 1975.
20. Z. Wang and X. Liu, *Nonlinear Dyn.* **95** (2019) 456.
21. M. Chen, X. Li, Y. Wang and B. Li, *Commun. Theor. Phys.* **67** (2017) 595.
22. X. Zhang and Y. Chen, *Commun. Nonlinear Sci. Numer. Simul.* **52** (2017) 24.
23. L. Huang and Y. Chen, *Commun. Theor. Phys.* **67** (2017) 473.
24. J. Y. Yang and W. X. Ma, *Int. J. Mod. Phys. B* **30** (2016) 1640028.
25. S. F. Tian and P. Ma, *Commun. Theor. Phys.* **8** (2014) 245.
26. D. Guo, S. F. Tian, X. B. Wang and T. T. Zhang, *Eur. Asian J. Appl. Math.* **9** (2019) 780.
27. X. W. Yan, S. F. Tian and X. B. Wang, *Int. J. Comput. Math.* **96** (2019) 1839.
28. C. Y. Qin, S. F. Tian, X. B. Wang, T. T. Zhang and J. Lin, *Comput. Math. Appl.* **75** (2018) 4221.
29. Y. Cao, J. He and D. Mihalache, *Nonlinear Dyn.* **91** (2018) 2593.
30. Y. Liu, B. Li and H. L. An, *Nonlinear Dyn.* **92** (2018) 2061.